Korean J. Chem. Eng., **21**(3), 721-725 (2004)

Photocatalytic Oxidation of Ethyl Alcohol in an Annulus Fluidized Bed Reactor

Myung-Jin Kim, Wooseok Nam and Gui Young Han†

Department of Chem. Eng., Sungkyunkwan University, Suwon 440-746, Korea
(*Received 9 April 2003 • accepted 15 January 2004*)

Abstract–The photocatalytic oxidation of ethyl alcohol vapor in an annulus fluidized bed reactor of 0.06 m I.D. and 1.0 m long was examined. The TiO_2 catalyst employed was prepared by the sol-gel method and was coated on the silica gel powder. The UV lamp was installed at the center of the bed as the light source. The effects of the initial concentration of ethyl alcohol, the power of UV-lamp, the photocatalysts with different preparation methods, and the superficial gas velocity on the reaction rate of ethyl alcohol decomposition were determined. It was found that, at 1.2 U_{mf} of flow rate, about 80% of ethyl alcohol was decomposed with initial concentration of 10,000 ppmv and the increase of superficial gas velocity reduced the reaction rate significantly.

Key words: Photocatalyst, TiO_2, Ethyl Alcohol, SiO_2, Sol-gel, Fluidized Bed

INTRODUCTION

The development of modern industry has rapidly improved the quality of human life, but has caused many problem concerned energy and environment. Therefore, it is not economic prosperity but the concerns with energy and environment that have seriously increased. At present, the regulation of air pollutant sources has been strict, and many studies to solve this problem have been conducted: for example advanced oxidation processes (AOP) by using photocatalysts. In particular, volatile organic compounds (VOCs) represented air pollutants are the most regulated air pollutant sources.

Since Fujisima and Honda reported the water splitting reaction using TiO_2 photoelectrodes in 1972, photocatalysis has been studying a variety of issues such as air or water pollutant treatment. Recently, studies of decomposition of VOCs by using UV-light have appeared [Braun et al., 1991; Fujishima et al., 2000; Rajeshwar and Ibanez, 1997; Schiasello, 1999].

Heterogeneous gas-solid photocatalysis is necessary to achieve both exposure of photocatalysts to UV-light and good contact between photocatalyst and reactant. Generally, packed bed reactors that used gas-solid reactions were difficult to penetrate into the interior of the reactor. But a fluidized bed photoreactor not only brings more contact of photocatalyst and gas but also enhances UV-light penetration through bubbles. Therefore, it is important to design a fluidized bed photoreactor having higher light throughput, large treatment of reactants and lower pressure drop [Lim et al., 2002; Nam et al., 1999].

Since the TiO_2 photocatalysts are usually a very fine powder (Geldart C type), the photocatalysts are easily entrained out of the bed by the up flow gas stream. Therefore, the use of relatively larger particles coated with photocatalysts can minimize entrainment; the appropriate support materials include porous silica, alumina and zeolites [Kunii et al., 1991; Cheremishinoff et al., 1984]. In this study, micro-porous silica gel has been selected as a support material since it has been used widely in industry, does not possess a changed framework, and is transparent to near UV-light [Xu et al., 1999].

In recent years, many works have dealt with the treatment of VOC and fluidized bed photoreactor. Sauer et al. [1996] treated photooxidation of ethanol in a recirculation reactor system with initial concentrations of 47-210 ppmv (90-400 mg m^{-3}) at all ethanol conversion. Lim et al. [2002] examined photodegradation of TCE with a fluidized bed. This system showed high conversion of TCE in a fluidized bed of TiO_2/silica-gel photocatalyst.

In this study, a gas-solid phase annulus fluidized bed reactor system was designed for the photocatalytic oxidation of organic contaminant compounds into a less hazardous substance. The photodegradation of ethyl alcohol was chosen to test for photocatalytic activity in the fluidized bed. The photocatalytic oxidation of ethyl alcohol is of interest because it is a pollutant from industrial processes such as in breweries and bakeries. The purpose of the present work is to determine the effect of parameters on the photocatalytic activity in the annulus fluidized bed.

EXPERIMENTAL

1. Preparation of TiO_2/SiO_2 Photocatalyst

The photocatalytic material used in this study was in the form of titanium hydroxide and/or TiO_2. Titanium hydroxides were derived via sol-gel hydrolysis precipitation of titanium tetra isopropoxide [$Ti(OC_3H_7)_4$]. At first, for TiO_2 photocatalyst preparation, the TTIP (99.9%, 28.4 ml) was slowly added into isopropyl alcohol (IPA 99.9%, 200 ml). Deionized water was lowly added under vigorous stirring conditions during 10 minutes. During the addition, a white precipitation [$Ti(OH)_4$] was formed. To compare the reactivity of photocatalyst prepared by sol-gel method, a commercial TiO_2 catalyst (Degussa P-25) was also prepared. The Degussa P-25 slurry solution was prepared by admixing 100 g of photocatalyst for 1,000 ml of deionized water. Then, these solutions were recontrolled of pH with admixing acid and/or base. SiO_2 (porous silica gel 60 : 0.2-0.5 μm) was employed as the support material. The porous SiO_2 powder was calcined at 573 K to clean the surface and pores of silica gel, and was added to the mixture for 1 hr. Through this treatment, the titanium dioxide particles were firmly bonded to the SiO_2 via

†To whom correspondence should be addressed.
E-mail: gyhan@skku.ac.kr

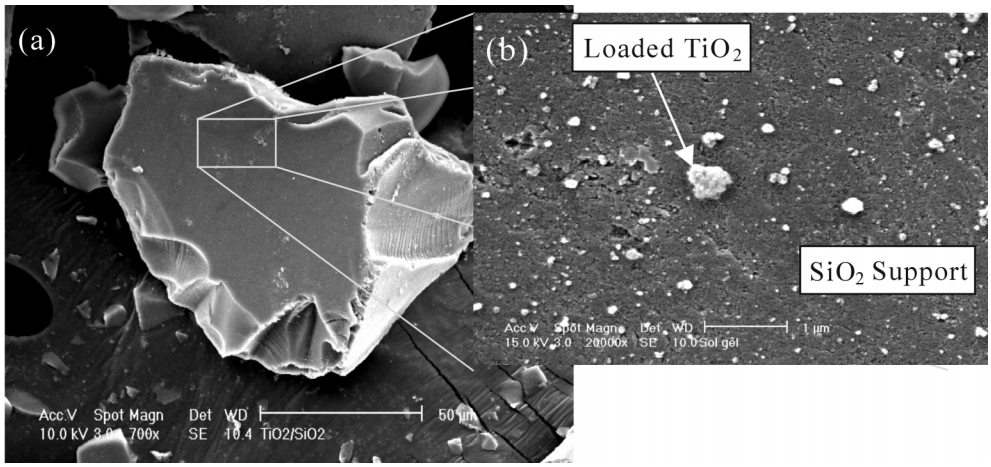

Fig. 1. SEM images of prepared TiO_2/SiO_2 photocatalyst: (a) overall image of particle (×700), (b) surface of photocatalyst (×20,000).

Van der Waals interaction and hydrogen bonding between hydroxylated titania surface and silica gel [Ackler et al., 1996]. Solids after the removal of solvent were heated to 363 K overnight and finally calcined at 773 K in open air for 1 hr. The polycrystalline TiO_2 size and shape of the obtained samples were observed by a scanning electron microscope (SEM). The SEM analysis confirmed the general morphologies of agglomerated TiO_2 powders.

Fig. 1 shows the dispersed TiO_2 powders prepared by the sol-gel method on the surface of SiO_2. The crystalline phases of prepared TiO_2/SiO_2 were analyzed by the powder X-ray diffraction analysis (XRD, Rigaku Co.) with nickel filtered CuK_α radiation (30 kV, 30 mA) and with the 2θ range from 20 to 80°. The scan speed was 10° min^{-1} and the time constant was 1 sec. The diffraction angle of 25.4° was selected to discuss the crystallinity of the prepared TiO_2. The XRD patterns of prepared TiO_2/SiO_2 powders prepared by sol-gel methods and slurry type are shown in Fig. 2.

Analysis of the XRD patterns revealed that the TiO_2/SiO_2 powders prepared by sol-gel method at different pH conditions successfully formed Ti-O-Si bonds through thermal treatment by the weak anatase phase pattern, and TiO_2 powders were not easily desorbed on the porous SiO_2 [Jung et al., 2001]. The XRD patterns showed a broad diffuse band similar to that of amorphous silica. This means that the TiO_2 and SiO_2 may be forming an amorphous mixture phase or two different phases of TiO_2 and SiO_2, and this trend was reported by Jung et al. [2001]. The morphological difference of TiO_2 catalysts by sol-gel method and the commercial slurry type TiO_2 photocatalyst was that Degussa P-25 showed the anatase and rutile phases, where TiO_2 catalyst prepared by the sol-gel method showed anatase phase only as shown in Fig. 2. The loaded amounts of TiO_2 with pH were shown in Fig. 3. As shown in Fig. 3, the loaded TiO_2 increased with pH up to 7 and reached a saturation value. During the admixture of SiO_2 at low pH condition, the amorphous TiO_2 precipitation agglomerated to the secondary powders. When the pH of the slurries was higher than pH 1, the amorphous TiO_2 sols were rapidly agglomerated to the secondary powders by OH· radicals [Nam et al., 2003].

In this study, because the photocatalysts were coated on the surfaces of porous silica gel, the TiO_2/SiO_2 photocatalysts employed

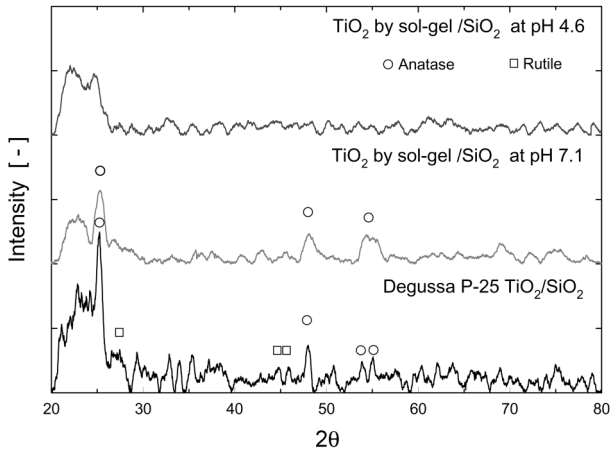

Fig. 2. XRD patterns of TiO_2/SiO_2 photocatalysts: (a) prepared at pH 4.2 by sol-gel method, (b) prepared at pH 7.1 by sol-gel method, and (c) prepared at pH 7 by admixing with Degussa P-25 slurry.

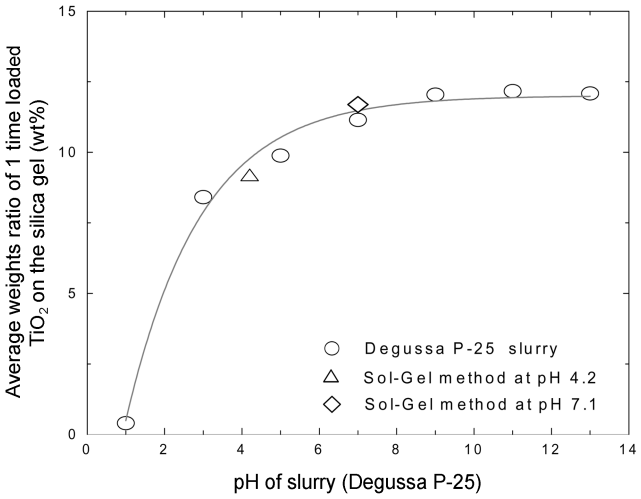

Fig. 3. The effect of pH on the weight of TiO_2 loaded on the silica gel.

were able to adsorb the reactant [Ruthven, 1984]. In fact, the ethanol vapors were removed by porous silica gel under dark run conditions. A 30 W black light lamp and a 65 W high pressure mercury lamp were used as the UV-source in this study, respectively, to determine the UV source effect on the reaction rates. The UV lamp was inserted in the cylindrical quartz tube to protect direct contact with gas and solid flow and located at the center of the bed. The increase of bed temperature was measured with a lamp to control the bed temperature. The bed temperature was increased up to 307 K for the 30 W lamp and 315 K for the 60 W lamp, respectively. It was assumed that this temperature rise does not affect the reaction rate. The TiO_2/SiO_2 photocatalysts employed are classified as Geldart B type particles, and it is expected that bubbles formed as soon as the gas velocity exceeds minimum fluidizing velocity (U_{mf}). Thus, these particles well fluidize a monotonous bubbling action and bubbles that grow large. The bed pressure drop (ΔP_b) is measured for the annulus fluidized bed photoreactor as a function of superficial gas velocity (U_g) for the TiO_2/SiO_2 photocatalysts. Experimentally, U_{mf} is determined about 0.67 cm/sec.

In this study, two different types of photocatalysts were employed: one prepared by sol-gel method at pH 7, and another admixed with Degussa P-25 slurry. The physical properties of these TiO_2/SiO_2 photocatalysts are shown in Table 1.

From the Table 1, it can be seen that the BET surface areas of the TiO_2/SiO_2 photocatalyst were more decreased than silica gel due to pore plugging by the impregnated TiO_2 [Lim et al., 2000].

2. Fluidized Bed Photoreactor

The schematic diagram of the experimental test set-up is shown in Fig. 4. The fluidized bed has an inside diameter of 0.06 m and is 1.0 m long and is made of acrylic pipe. The UV lamp was installed at the center of the reactor through the inside of the quartz tube of 0.03 m O.D. and 1.0 m long and reactant gases (air and ethanol vapor) flowed through the annulus region of the bed as shown in Fig. 4. The liquid ethanol was vaporized by air bubbling at the vaporizer and mixed with air and flowed into the bed at designed concentration and flow rates. Two flow-meters were used to control the flow rates of ethanol vapor and air, respectively. The entrained particles were separated by cyclone separator and bag filter. A high concentration of ethanol vapor was employed to enhance the reaction rates. The sampling of the inlet gas and outlet gas was done with a gas-tight syringe every 30 min, and the gas composition was determined by gas chromatograph and mass spectroscope.

Table 1. Physical properties of TiO_2/SiO_2 photocatalysts

Properties \ Type	SiO_2	TiO_2/SiO_2 pH 7	TiO_2/SiO_2 degussa
ρ_s (g/cm^3)	1.98	2.14	2.19
d_p (μm)		112	
Φ_s		0.67	
Geldart classification		B-type	
Heat treatment (K/1 hr)	573	773	
Crystalline structure	amorphous	Anatase	Anatase : Rutile 7 : 3
Weight ratio (TiO_2/SiO_2)	0	0.12	0.13
B.E.T. surface area (m^2/g)	512	462	432

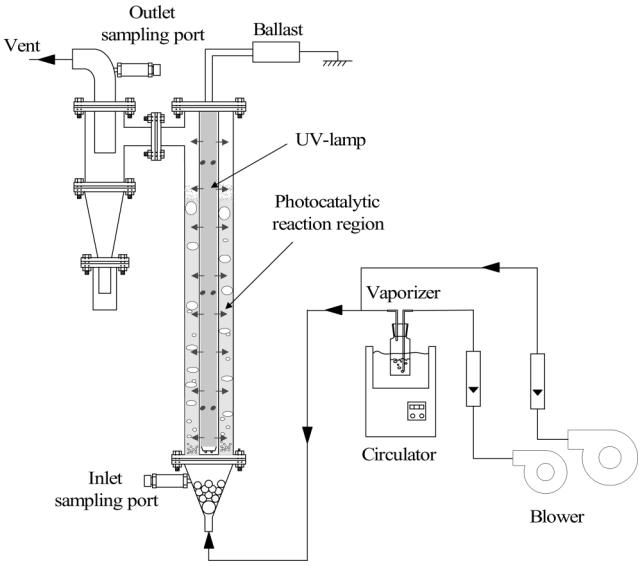

Fig. 4. Schematic diagram of the fluidized bed photoreactor system.

RESULT AND DISCUSSION

1. Effects of Gas Flow Rate and Light Intensity

The prepared TiO_2/SiO_2 photocatalysts of 800 g were charged to the reactor and a feed stream of 10,000 ppmv (0.41 mole m^{-3}) of ethyl alcohol vapor was fed to the reactor through the annular region in the bed. The gas flow rate of ethanol vapor was controlled at 1.2, 1.5 and 2.0 U_{mf}, respectively. The effects of gas flow rates and UV source intensity on the photocatalytic oxidation of methanol vapor in the fluidized bed are shown in Fig. 5. As can be seen in Fig. 5, the increase of gas flow rates decreased the reaction rates. As the gas flow rate increased over 1.2 U_{mf} (0.84 cm sec^{-1}), the average reaction rate sharply decreased due to the increase of by-passing gas flow. Since the gas flow in the bubble phase cannot effectively contact with photocatalysts, it resulted in a decrease of reaction rate. Furthermore, at higher gas flow rates, the shorter residence time of

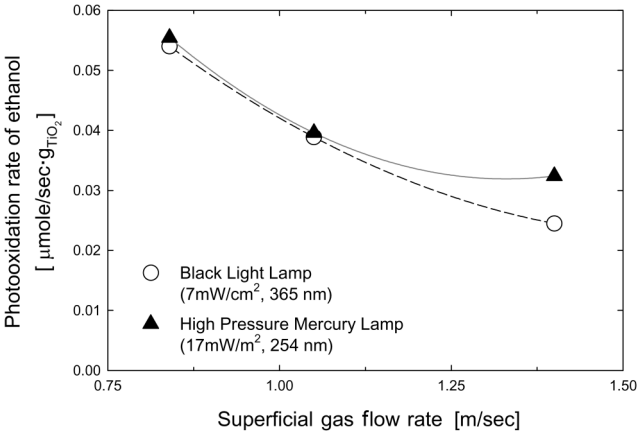

Fig. 5. Effect of gas velocity on the photooxidation rates of ethanol using the prepared TiO_2/SiO_2 photocatalysts (TiO_2/SiO_2 800 g, T=30 C, C_o=10,000 ppmv).

reactant gases in the bed would decrease the reaction rate. Therefore, for the above-mentioned two reasons, the increased gas flow rates decreased the reaction rates significantly. On the other hand, the effect of UV lamp intensity is somewhat different. At lower gas flow rates, the effect of UV lamp intensity was negligible. However, at the higher gas flow rate condition, the effect of UV lamp intensity was clear. Because at higher gas flow rate, bubble phase flow was increased and light transmission through the bubbles would be the important factor in determining the reaction rate. The intensity of 30 W UV BL lamp is 7 mW/cm^2 and 65 W LPM lamp is 17 mW/cm^2. And the strong energy of short wave length (254 nm) penetrated into the photocatalytic reaction region of the reactor through the voidage [Raupp et al., 1997]. Therefore, the 65 W LPM lamp was more effective in transmitting the UV light through the bubbles. It has been also reported that the shorter wavelength of 254 nm radiation is more effective than wavelength of 350 nm for TiO_2 without loading on SiO_2 [Matthews et al., 1992].

2. Effect of Initial Concentration of Ethanol Vapor and Light Intensity

Since the photocatalytic reaction is governed by photon efficiency and mass transfer limitation, the mechanism is quite different with conventional heterogeneous catalytic reaction. The effects of initial concentration of ethanol vapor on the rate of photo-catalytic conversion and light intensities are shown in Fig. 6. As the initial concentration of ethanol vapor was increased, the average photooxidation rate steadily increased to about 30,000 ppmv (1.22 mole m^{-3}) and then the photooxidation rates almost reached a steady value. This is because the reactants were plentifully presented surrounding the photocatalyst and photoactivated sites were easily contacted with reactants. However, the concentration of reactant was very higher; it seems that the treatment capacity of photocatalysts was in the vicinity of a limit and photoactivated sites were occupied by intermediates such as acetaldehyde, formaldehyde and acetic acid etc. Over the limit, photocatalytic conversion rate will be decreased. Thisw was reviewed by Zhao et al., [2003].

3. Effect of the Photocatalysts with Different Preparation Methods

The crystal structures of TiO_2 are reported to have powder structures of anatase, rutile and brookite. Mainly, the structures of anatase and rutile are employed in the photocatalysis. Generally, anatase powder was found to be photocatalytically more active than rutile [Karl et al., 1990; Lee et al., 1999]. The influence of the preparation method on the photo activities was studied at the same conditions, as shown in Fig. 7.

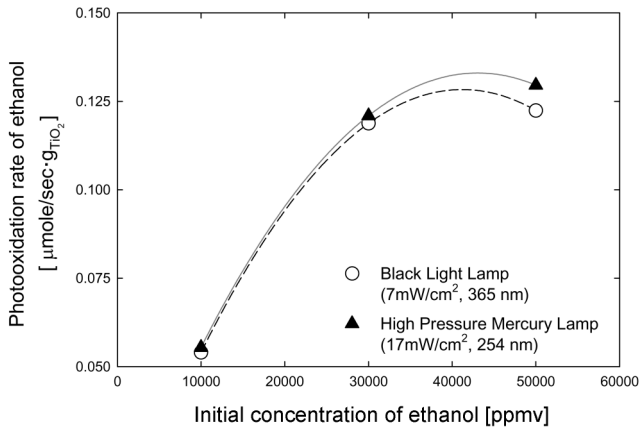

Fig. 6. Effect of initial concentration on the photooxidation rate of ethanol using the prepared TiO_2/SiO_2 photocatalysts (TiO_2/SiO_2 800 g, U=1.2 U_{mf}, T=30 C).

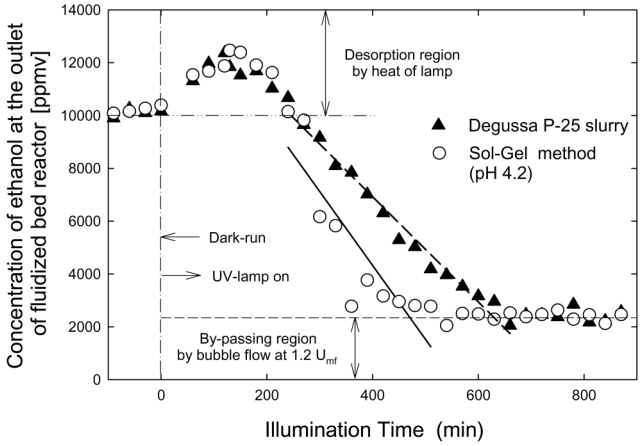

Fig. 7. Effect of photocatalysts type on the photooxidation rate of ethanol (TiO_2/SiO_2 800 g, U=1.2 U_{mf}, T=30 C, C_o=10,000 ppmv).

The initial photocatalytic oxidation rate differed with the preparation methods of photocatalysts. As can be seen in Fig. 7, the photocatalyst prepared by sol-gel method showed higher oxidation rate than that of P-25 slurry type photocatalyst. Based on the concentration decrease interval from 10,000 ppm to 3,000 ppm, the sol-gel method catalyst showed about 30-50% higher reaction rate than the commercial catalyst (P-25). However, the steady state photooxidation rate which was obtained after 6 hrs run was almost the same. From this result, it can be said that the activity of photocatalyst prepared by the sol-gel method was higher than that of Degussa P-25, and this higher activity may be resulting from the increased active sites on the larger surface area of prepared TiO_2/SiO_2 by the sol-gel method.

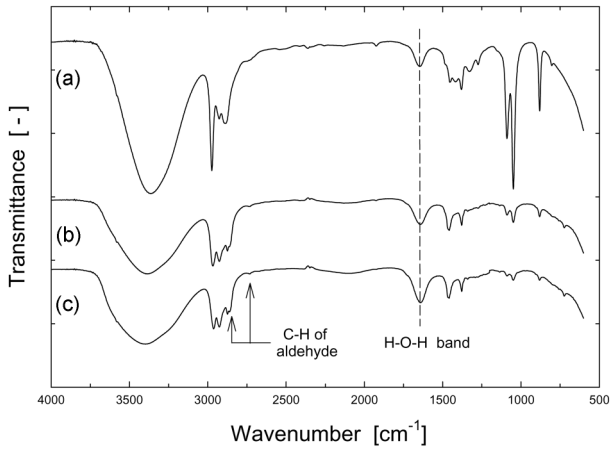

Fig. 8. FTIR spectra of photocatalyst after dark-run and photocatalytic reaction: (a) 6-hrs dark- run (b) photocatalytic oxidation with TiO_2/SiO_2 by admixing with Degussa P-25 slurry (c) photocatalytic oxidation with TiO_2/SiO_2 by sol-gel method.

After photocatalytic reaction, the by-products of photooxidation of ethanol vapor were analyzed by FTIR. Fig. 8 shows the IR spectra of adsorbed organic compounds on TiO_2 after 6-hrs dark-run experiment and 6-hrs photocatalytic reaction, respectively. For the samples at 307 K, strong absorption bands of H-O-H at 1,637 cm^{-1}, broad bands of 3,400-3,300 cm^{-1}, and C-H bands of aldehyde at 2,850, 2,750 cm^{-1} were observed [Lim et al., 2002; Skoog et al., 1998]. From this result, it may be concluded that major by-products of photo-degradation of ethanol were aldehyde compounds, and the recirculation of exit gases is required to complete photooxidation of ethanol into carbon dioxide and water.

CONCLUSIONS

The high concentration of ethanol vapor was oxidized in the fluidized bed photocatalytic oxidation system in order to take advantages of fluidized bed system.

The fluidized bed reactor gives effective contact between the reactant gases and photocatalysts and direct and close illumination of the UV-source on the photocatalysts. From a parameter study of photocatalytic oxidation of ethanol, it was found that the reaction rate decreased with gas flow rates due to by-pass bubble formation and short residence time, and the short wave length of UV source was more effective in transmitting the UV light through the bubbles. The reaction rate increased with initial concentration of ethanol vapor and then reached a steady state value. The photocatalyst prepared by sol-gel method showed higher photocatalytic activity than that with Degussa P-25 catalyst. Finally, the major by-products of ethanol vapor during photocatalytic reaction were aldehyde compounds.

ACKNOWLEDGMENTS

This work was supported by grant R01-2003-000-10028-0 from the Basic Research Program of the Korea Science & Engineering Foundation.

REFERENCES

Acker, H. D., French, R. H. and Chiang, Y. M., "Comparisons of Hamaker Constants for Ceramic Systems with Intervening Vacuum or Water: from Force Laws and Physical Properties," *J. Coll. Interf. Sci.*, **179**, 460 (1996).

Braun, A. M., Maurette, M. and Oliveros, E., "Photochemical Technology," John Wiley & Sons, New York, 107 (1991).

Cheremishinoff, N. P. and Cheremisinoff, P. N., "Hydrodynamics of Gas-solids Fluidization," Gulf Publishing Company, Houston, 137 (1984).

Fujishima, A., Rao, T. N. and Tryk, D. A., "Titanium Dioxide Photocatalysis," *J. Photochem Photobiol., C*, **1**, 1 (2002).

Jung, S. M., Dupont, O. and Grange, P., "TiO_2-SiO_2 Mixed Oxide Modified with H_2SO_4. Characterization of the Microstructure of Metal Oxide and Sulfate," *Appl. Catal., A:gen.*, **208**, 393 (2001).

Karl, M. S. and Marinus, K., "Charge-carrier Dynamics in TiO_2 Powder," *J. Phys. Chem.*, **94**, 8222 (1990).

Kunii, D. and Levenspiel, O., "Fluidization Engineering," Butterworth-Heinemann, Boston, 71 (1991).

Lee, Y. D., Ahn, B. H., Lim, K. T., Jung, Y. T., Lee, G. D. and Hong, S. S., "Photocatalytic Degradation of Trichloroethylene over Titanium Dioxide," *J. Korean Ind. Eng. Chem.*, **10**, 1035 (1999).

Lim, T. H., Jeong, S. M., Kim, S. D. and Gyenis, J., "Photocatalytic Decomposition of NO by TiO_2 Particle," *J. Photochem. Photobiol. A: Chem.*, **134**, 209 (2000).

Lim, T. H. and Kim, S. D., "Photocatalytic Degradation of Trichloroethylene over TiO_2/SiO_2 in an Annulus Fluidized Bed Reactor," *Korean J. Chem. Eng.*, **19**, 1072 (2002).

Matthews, R. W. and Mxevoy, S. R., "A Comparison of 254 nm and 350 nm Excitation of TiO_2 in Simple Photocatalytic Reactors," *J. Photochem. Photobiol. A: Chem.*, **66**, 355 (1992).

Nam, W., Kim, J. and Han, G., "Photocatalytic Oxidation of Methyl Orange in a Three-phase Fluidized Bed Reactor," *Chemosphere*, **47**, 1019 (2002).

Nam, W. and Han, G., "A Photocatalytic Performance of TiO_2 Photocatalyst Prepared by the Hydrothermal Method," *Korean J. Chem. Eng.*, **20**, 180 (2003).

Raupp, G. B., Nico, J. A., Annangi, S., Changrani, R. and Annapragada, R., "Two-Flux Radiation-Filed Model for an Annular Packed-Bed Photocatalytic Oxidation Reactor," *AIChE J.*, **43**, 792 (1997).

Ruthven, D. M., "Principles of Adsorption and Adsorption Processes," John Wiley & Sons, New York, 5 (1984).

Sauer, M. L. and Ollis, D. F., "Photocatalyzed Oxidation of Ethanol and Acetaldehyde in Humidified Air," *J. Catal.*, **158**, 570 (1996).

Schiavello, M., "Wiley Series in Photoscience and Photoengineering: Heterogeneous Photocatalysis," Wiley, 169 (1999).

Skoog D. A., Holler F. J. and Nieman T. A., "Principles of Instrumental Analysis," Saunders colleges publishing, Philadelphia, 404 (1998).